Hindawi
Journal of Mathematics
Volume 2023, Article ID 2050684, 20 pages
https://doi.org/10.1155/2023/2050684

Research Article

Optimal Control Strategies of COVID-19 Dynamics Model

Temesgen Duressa Keno and Hana Tariku Etana

Department of Mathematics, Wallaga Univesity, Nekemte, Ethiopia

Correspondence should be addressed to Temesgen Duressa Keno; temesgenduressaa@gmail.com

Received 12 December 2022; Revised 26 December 2022; Accepted 16 January 2023; Published 16 February 2023

Academic Editor: Niansheng Tang

In this paper, we proposed the optimal control for the dynamics of COVID-19 with cost effectiveness strategies. First, we showed that model solution is positive, and bounded in a fixed domain. Besides, we used next-generation matrix to compute the basic reproduction number. If the basic reproduction number is less than one, then the disease-free equilibrium point is both locally and globally stable, respectively, via the help of Jacobian matrix and Lyapunov function, otherwise the endemic equilibrium occurs. The sensitivity analysis was determined with regard to all basic parameters. Then the model is fitted with COVID-19 infected cases reported from October 1, 2022 to October 30, 2022 in Ethiopia. The values of model parameters are then estimated from the data reported using the least-square method. Furthermore, using Pontryagin maximum principle, the model is extended to optimal control incorporating three control namely: personal protective, vaccination, and treatment of infected humans. Finally, based upon the numerical simulation of optimal controls and cost effectiveness analysis, the most optimal and less costly strategy to minimize the disease is combination of vaccination and treatment of infected.

1. Introduction

The World Health Organization (WHO) declared COVID-19 to be a pandemic of international concern after the first human cases of the disease were reported by authorities in Wuhan City, China, in December 2019. As of June 1, 2022, More than 530 million infections and over 6.2 million people deaths had been caused worldwide by the virus, according to [1]. In India, the second COVID-19 wave has been extremely severe, with more than 30,000 new cases being confirmed every day during the final week of April 2021. The WHO reports that as of December 15, 2022, there have been 646,740,524 confirmed cases of COVID-19 and more than 6,637,512 deaths [2]. The first COVID-19 case to be reported in Africa occurred in Egypt on February 14, 2020. In Africa, there have been a total of 627,104,342 confirmed cases, 6,567,552 fatalities as of October 31, 2022 [2]. The first case of COVID-19 in Ethiopia was identified on March 13, 2020, in Addis Ababa, the country's capital. Then on October 30, 2022, the Ethiopian Public Health Institute reported a total of 493,940 confirmed cases [1]. Sadly, this virus was able to spread very quickly, which increased the number of deaths each day. Therefore, it is crucial to stop the disease from spreading using non-drug methods like confinement. Due to COVID-19's novelty, there is currently no known treatment. The disease is being treated, though, with the development of vaccines and antivirals. As the immune system of the infected person fights the virus, current case management focuses on reducing disease symptoms. It should be noted that COVID-19 complications are more likely to affect older people and people with underlying medical conditions like lung disease, asthma, cancer, diabetes, liver disease, and other immune compromised conditions [3]. The novel coronavirus disease can be prevented by adhering to measures, including regular hand washing or use of alcohol-based sanitizer, maintaining social distancing, avoiding crowded places, use of face masks, and use of hand gloves with personal protective clothing by healthcare workers while giving care to COVID-19 patients [3].

A number of researchers have studied the modeling and an optimal control of COVID-19 transmission model to determines the role of control measures on disease transmission. For instance, Oke et al. [4] a mathematical model

that has been proposed to investigate the COVID-19 outbreak in Africa. A system of differential equations makes up the model. The author's findings lead to an increase in case detection and a decrease in the burden of the novel corona virus in Africa. Yang et al. [5] a mathematical model is presented to investigate the effect of vaccination on the spread of the COVID-19 virus. The authors recommended reducing contacts and vaccinating people to control COVID-19 diseases. Abriham et al. [6] the author proposed SEQ$I_S I_N$HR compartmental model with the impact of prevention and control measures. The author comes to the conclusion that increasing isolation and quarantine rates will control COVID-19 disease. Noah and Kabir [7] presented a SEIHR compartmental non-linear deterministic epidemic model for COVID-19 transmission dynamics. The authors propose that social withdrawal, wearing a face mask in public, and isolating infected people are effective combinations for lowering COVID-19 diseases. Ahmed et al. [8] the author presented a mathematical model and method for controlling a novel coronavirus using fractional derivatives and ordinary differential equations. The authors recommended limiting contact between those who were exposed and those who were vulnerable. DarAssi et al. [9] studied a mathematical model for transmission dynamics of COCID-19. The authors concluded that the combination of vaccination, isolation and detection is the best strategies to mitigate the disease. Peter et al. [10], formulated a mathematical model for controlling a novel coronavirus in Pakistan. The authors fitted the parameter values for a using the quantity of real cases from Pakistan. The authors demonstrated that a controlled rate of transmission can decrease the pandemic of the disease.

Mbogo et al. [11] presented a mathematical model for transmission of COVID-19 epidemic. The author conclude that reduce the contact between susceptible and exposed populations can minimize the spread of the disease. Khajanchi et al. [12] developed COVID-19 SEIR compartment mathematical modeling. The author used social distances and isolation of effectiveness to control novel corona virus disease. Goswami and Shanmukha [13] a non-linear mathematical model was used to examine how the COVID-19 pandemic's dynamics of transmission affected India. Additionally, they transformed the suggested model into an optimal control model. According to the authors, models with optimal control have more consistent results when it comes to lowering the number of infected people when compared to models without optimal control. Nana-Kyere and Sacrifice [14] studied the SEIRW COVID-19 compartmental model by extending to the optimal control model using three control measures. They come to the conclusion that a combination of personal protection, drug treatment and spraying considered by significantly reducing the number of exposed and infected people in the population. Seidu [15] presented optimal strategies for control of COVID-19 using deterministic ordinary differential equations. The authors conclude that controlling the spread of COVID-19 through physical distance and use face mask is the most effective strategy. Adesoye et al. [16] discussed dynamic COVID-19 and its optimal control by incorporating three control strategies. The authors suggested that mixed of three controls such as use of face mask and hand sanitizer with social distancing, treatment of COVID-19 patient and control against recurrence to reduce COVID-19 in Nigeria.

Moore and Eric [17] has investigated four control mechanisms for preventing the spread of the corona virus: personal protection, hospitalization and treatment with early diagnosis, hospitalization and treatment with delayed diagnosis, environmental spraying, and cleaning of potentially infected surfaces. The authors come to the conclusion that quarantine and medical care for infected can minimize the transmission risk and mortality rates. Obsu and Balcha [18] non-linear ordinary differential equations were used to study the transmission risk of COVID-19 with the best possible control by applying three control measures. The authors come to the conclusion that medical care and intensive prevention are good control measures to reduce the number of populations that are exposed and infected. Asamoah et al. [19] proposed a COVID-19 model to study how to control the spread of the corona virus in Saudi Arabia using four control measures, including personal hygiene, proper safety precautions, practicing proper protocol, and fumigating schools. In the absence of vaccination, the author's conclusion is that implementing physical or social distance protocols is the most effective and cost-efficient control intervention. Maryam [20] presented a compartment of the SEIR model with the optimal control problem using two control measures for COVID-19 transmission. In order to reduce COVID-19, the author suggests a combination of two control measures: vaccination and health education. Deressa and Duressa [21] investigated the SEIR model of COVID-19 transmission dynamics with ideal control to hospitalized and asymptomatic individuals. Using actual data from Ethiopia, the author estimated the parameter value. They come to the conclusion that a combination of three factors, including personal protection, public health education, and COVID-19 infection treatment, can reduce the number of coronavirus infections. Li et al. [22] developed a COVID-19 model with three control measures for optimal control. The authors concluded that the combination of vaccination, isolation and detection is the best strategies to mitigate the disease. Olaniyi et al. [23] the formulated optimal control of COVID-19 dynamics using Pontryagin maximum principle with different controls strategies. Finally, they conclude that these controls can reduce the prevalence of COVID-19 in the population.

All of these studies, however, did not analyze the COVID-19 vaccine epidemic optimal control model with cost effectiveness analysis. In this paper, the model [24] is extended to the optimal control with cost effectiveness strategies. Moreover, the parameters are estimated using real data of confirmed cases from October 1, 2022 to October 30, 2022 in Ethiopia.

This paper is arrange as follows: mathematical model is discussed in Section 2. The model of analysis is describe in Section 3. Sensitivity analysis has been discussed in Section 4. By using Pontryagin maximum principle, the optimal control of the COVID-19 transmission model is analytically

analyzed in Section 5. We show the numerical simulation in Section 6. The analysis of cost effectiveness is depicted in Section 7. Finally, in Section 8 we summary and discussion of the results.

2. Model Formulation and Description

The model formulate for the COVID-19 transmission is subdivided into five classes: Susceptible $S(t)$, Exposed $E(t)$, Infected $I(t)$, hospitalized $H(t)$ and Recovered $R(t)$ Classes. Thus, the size of total population is given as $N(t) = S(t) + E(t) + I(t) + H(t) + R(t)$. The susceptible human population class is created by the recruitment rate π through birth and immigration, leaves by having active contact at the rate β, and also decreases by natural death at the rate μ. These people move up to exposed class $E(t)$. When an exposed person exhibits clinical symptoms, they are moved into the infected class $I(t)$ at a rate of δ, which causes the exposed class to decrease. Additionally, it decreases at rates of μ, σ, and τ_1, respectively, through natural death, disease-related death, and recovery from early intervention (treatment). The population of infected people decreases due to hospitalization at a rate of θ, natural death at a rate of μ, and disease-related death at a rate of σ. The number of patients in hospitals increase when infected people move there at a rate of θ and decreases when people die naturally at a rate of μ. Additionally, it decreases through COVID-19-related deaths at a rate of σ and recovery at a rate of τ_2. The population of the recovered class increase whenever the exposed class recovers from early treatment at rates of τ_1, as well as when hospitalized patients recover from treatment after being hospitalized at rates of τ_2, and it decreases due to natural death. The recovered individuals become again susceptible to the disease with at rate of ω. Figure 1 shows the flow diagram of COVID-19 and the description of all parameters are listed in Table 1.

Based on the above diagram, the description of the dynamics of the COVID-19 disease is depicted by following set of equations:

$$\begin{cases} \dfrac{dS}{dt} = \pi - \beta IS - \mu S + \omega R, \\ \dfrac{dE}{dt} = \beta IS - (\delta + \sigma + \mu + \tau_1)E, \\ \dfrac{dI}{dt} = \delta E - (\theta + \sigma + \mu)I, \\ \dfrac{dH}{dt} = \theta I - (\tau_2 + \sigma + \mu)H, \\ \dfrac{dR}{dt} = \tau_1 E + \tau_2 H - (\mu + \omega)R, \end{cases} \tag{1}$$

with initial conditions

$$\begin{aligned} S(0) &= S_0, \\ E(0) &= E_0, \\ I(0) &= I_0, \\ H(0) &= H_0, \\ R(0) &= R_0. \end{aligned} \tag{2}$$

3. Mathematical Analysis of the Model

3.1. Invariant Region. Invariant region is used to determine in which the solution of the model is bounded.

Theorem 1. *The closed region* $\Omega = \{(S, E, I, H, R) \in R_+^5 : N(t) \le \pi/\mu\}$ *is positive invariant set for the model (1).*

Proof. Let the total population $N(t)$ at any time t is given by

$$N(t) - = S(t) + E(t) + I(t) + H(t) + R(t). \tag{3}$$

Differentiation of (3), with respect to t gives

$$\frac{dN}{dt} = \pi - \mu N - (E + I + H)\sigma. \tag{4}$$

This implies that

$$\frac{dN}{dt} \le \pi - \mu N. \tag{5}$$

Integrating the (5), we obtain

$$\pi - \mu N(t) \ge (\pi - \mu N(0))e^{-\mu t}. \tag{6}$$

By taking limit as $t \longrightarrow \infty$ on the inequality (6), we get

$$N(t) \le \frac{\pi}{\mu}. \tag{7}$$

Therefore, all the state variables with the initial values given in (1) for the human population are given by

$$\Omega = \left\{(S, E, I, H.R) \in R_+^5 : 0 \le N(t) \le \frac{\pi}{\mu}\right\}, \tag{8}$$

which is the set of feasible solutions for the model (1), all of which are contained within it, and we draw the conclusion that the model (1) is mathematically and epidemiologically well-posed within Ω [25]. □

3.2. Positivity and Boundedness

Theorem 2. *Let* $S(0)$, $E(0)$, $I(0)$, $H(0)$ *and* $R(0)$ *be non negative initial conditions, then the solutions* $(S(t), E(t), I(t), H(t), R(t))$ *of the proposed model in (1) are positive for all* $t > 0$.

Proof. Consider the following from the model's first equation (1)

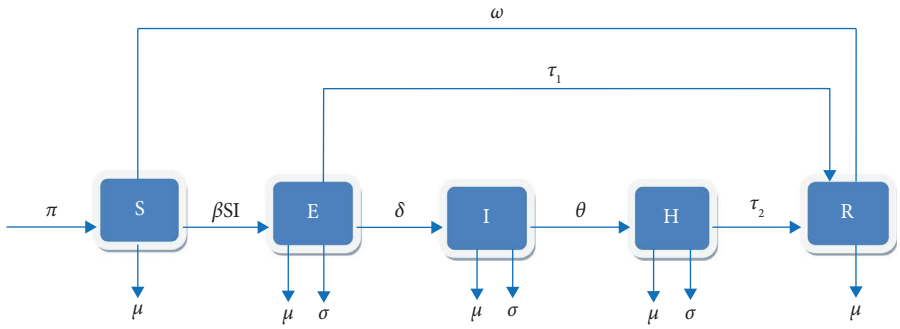

Figure 1: Flow diagram of COVID-19 transmission dynamics.

Table 1: Parameters description used for the model (1).

Parameters	Parameters description
π	Human recruitment rate
β	Probability of contact rate transmission
τ_1	Early intervention recovery rate
θ	Hospitalization rate of infected people
δ	Rate at which those who have been exposed become infected
μ	Natural deaths rate of human
τ_2	The proportion of hospitalized patients who recover
σ	Rate of COVID-19-related deaths
ω	Rate of recovered individuals to be again susceptible class

$$\frac{ds}{dt} = \pi - (\beta I + \mu)S + \omega R. \tag{9}$$

This is true that

$$\frac{dS}{dt} \geq -(\beta I + \mu)S. \tag{10}$$

Integrating (10) using the method of separating the variables by applying the initial condition when solving with respect to time, we obtain

$$S(t) \geq S(0)e^{-(\beta I+\mu)t} > 0. \tag{11}$$

Using the same justification, we can demonstrate that

$$E(t) \geq E(0)e^{-(\tau_1+\delta+\sigma+\mu)t} > 0, \quad I(t) \geq I(0)e^{-(\theta+\sigma+\mu)t} > 0, \; H(t) \geq H(0)e^{-(\tau_2+\sigma+\mu)t} > 0, \; R(t) \geq R(0)e^{-(\omega+\mu)t} > 0. \tag{12}$$

This demonstrates that system (1) solution is positive for all $t > 0$. As a result, the suggested model (1) is epidemiologically significant and mathematically well posed in the domain Ω [25]. □

3.3. Disease Free Equilibrium (DFE). In the absence of the COVID-19, the model has a COVID-19 free equilibrium that represents the system's critical points (1). At $I(t) = 0$, we set the left side of model (1) equal to zero in order to determine the DFE. By using the symbol E_0 to stand for the disease-free equilibrium point and solving for the non-infected state variable, the disease-free equilibrium point is obtained.

$$\begin{aligned} E_0 &= \left(S^0, E^0, I^0, H^0, R^0\right) \\ &= \left(\frac{\pi}{\mu}, 0, 0, 0, 0\right). \end{aligned} \tag{13}$$

3.4. Basic Reproduction Number (R_0). In this section, the basic reproduction number, denoted by R_0, is defined as the average amount of secondary infectious caused by primary infection in the given period [26]. We use the next-generation matrix method to compute reproduction number population classes. The first step is rewrite the model (1), by starting the infected human, exposed and hospitality population classes.

$$\begin{aligned}\frac{dE}{dt} &= \beta SI - (\delta + \sigma + \mu + \tau_1)E,\\ \frac{dI}{dt} &= \delta E - (\theta + \sigma + \mu)I,\\ \frac{dH}{dt} &= \theta I - (\tau_2 + \sigma + \mu).\end{aligned} \tag{14}$$

The right-hand side of system (11) for this model can be expressed as f-v, where

$$\begin{aligned}f &= \begin{bmatrix}\beta SI\\ 0\\ 0\end{bmatrix},\\ v &= \begin{bmatrix}(\tau_1 + \delta + \sigma + \mu)E\\ (\theta + \sigma + \mu)I - \delta E\\ (\tau_2 + \sigma + \mu) - \theta I\end{bmatrix}.\end{aligned} \tag{15}$$

The Jacobian matrices at F and V disease-free equilibrium point are obtained by taking a partial derivative with respect to E, I and H as follows:

$$\begin{aligned}F &= \begin{bmatrix}0 & \beta\dfrac{\pi}{\mu} & 0\\ 0 & 0 & 0\\ 0 & 0 & 0\end{bmatrix},\\ V &= \begin{bmatrix}(\tau_1 + \delta + \sigma + \mu) & 0 & 0\\ -\delta & (\theta + \sigma + \mu) & 0\\ 0 & -\theta & (\tau_2 + \sigma + \mu)\end{bmatrix},\\ V^{-1} &= \begin{bmatrix}\dfrac{1}{(\tau_1 + \delta + \sigma + \mu)} & 0 & 0\\ \dfrac{\delta}{(\tau_1 + \delta + \sigma + \mu)(\theta + \sigma + \mu)} & \dfrac{1}{(\theta + \sigma + \mu)} & 0\\ \dfrac{\theta\sigma - (\theta + \sigma + \mu)}{(\tau_1 + \delta + \sigma + \mu)(\theta + \sigma + \mu)(\tau_2 + \sigma + \mu)} & 0 & \dfrac{1}{(\tau_2 + \sigma + \mu)}\end{bmatrix}.\end{aligned} \tag{16}$$

Moreover, the product of FV^{-1} is obtain as:

$$FV^{-1} = \begin{bmatrix}\dfrac{\beta\pi\delta}{\mu(\tau_1 + \delta + \sigma + \mu)(\theta + \sigma + \mu)} & \dfrac{\beta\pi}{\mu(\theta + \sigma + \mu)} & 0\\ 0 & 0 & 0\\ 0 & 0 & 0\end{bmatrix}. \tag{17}$$

Given that F is non-negative and V is non-singular, V^{-1} and FV^{-1} are both non-negative. The matrix FV^{-1} is referred to as the model's next-generation matrix [27]. It is possible to calculate the eigenvalues of the matrix FV^{-1} as $\det(FV^{-1} - \lambda) = |FV^{-1} - \lambda| = 0$. This implies.

$$\left|FV^{-1} - \lambda\right| = \begin{vmatrix} \dfrac{\beta\pi\delta}{\mu(\tau_1 + \delta + \sigma + \mu)(\theta + \sigma + \mu)} - \lambda & \dfrac{\beta\pi}{\mu(\theta + \sigma + \mu)} & 0 \\ 0 & 0 - \lambda & 0 \\ 0 & 0 & 0 - \lambda \end{vmatrix} = 0. \tag{18}$$

Final from (18), the basic reproduction number, $R_0 = \rho(FV^{-1})$ is the largest eigenvalue of the product FV^{-1} and given as:

$$R_0 = \frac{\delta\beta\pi}{\mu(\tau_1 + \mu + \delta + \sigma)(\theta + \sigma + \mu)}. \tag{19}$$

3.5. Local Stability of Disease Free-Equilibrium

Theorem 3. *The disease free-equilibrium point of system (1) is locally asymptotically stable in* Ω *if* $R_0 < 1$.

Proof. The system's Jacobian matrix of model (1) is calculated as

$$J(E_0) = \begin{pmatrix} -(\beta I + \mu) & 0 & -\beta S & 0 & \omega \\ \beta I & -(\tau_1 + \delta + \sigma + \mu) & \beta S & 0 & 0 \\ 0 & \delta & -(\theta + \sigma + \mu) & 0 & 0 \\ 0 & 0 & \theta & -(\tau_2 + \sigma + \mu) & 0 \\ 0 & \tau_1 & 0 & \tau_2 & -(\mu + \omega) \end{pmatrix}. \tag{20}$$

The Jacobian matrix at DFE $E_0 = ((\pi/\mu), 0, 0, 0, 0)$ of system (1) is given as

$$J(E_0) = \begin{pmatrix} -\mu & 0 & -\beta\left(\dfrac{\pi}{\mu}\right) & 0 & \omega \\ 0 & -(\tau_1 + \delta + \sigma + \mu) & \beta\left(\dfrac{\pi}{\mu}\right) & 0 & 0 \\ 0 & \delta & -(\theta + \sigma + \mu) & 0 & 0 \\ 0 & 0 & \theta & -(\tau_2 + \sigma + \mu) & 0 \\ 0 & \tau_1 & 0 & \tau_2 & -(\mu + \omega) \end{pmatrix}. \tag{21}$$

From (21), the corresponding characteristic equation has the following form:

$$(-\mu-\lambda)(-\lambda-(\mu+\omega))(-(\tau_2+\sigma+\mu)-\lambda)\left(\lambda^2+b_1\lambda+b_2\right)=0, \quad (22)$$

where

$$\begin{aligned} b_1 &= (\tau_1+\delta+\sigma+\mu)+(\theta+\sigma+\mu),\\ b_2 &= (\tau_1+\delta+\sigma+\mu)(\theta+\sigma+\mu)-\frac{\delta\pi\beta}{\mu}. \end{aligned} \quad (23)$$

From (22), we obtain that

$$\begin{aligned} \lambda_1 &= -\mu<0,\\ \lambda_2 &= -(\mu+\omega)<0,\\ \lambda_3 &= -(\tau_2+\sigma+\mu)<0, \end{aligned} \quad (24)$$

and from the last characteristic equation, we have

$$\lambda^2+b_1\lambda+b_2=0. \quad (25)$$

By applying the Routh-Hurwitz criteria [28], equation (25) has a real root that is strictly negative if $b_1>0$ and $b_2>0$. Due to the fact that b_1 is the sum of positive parameters, we can see that $b_1>0$, we have

$$b_2=(\tau_1+\delta+\sigma+\mu)(\theta+\sigma+\mu)-\frac{\delta\pi\beta}{\mu}=1-R_0. \quad (26)$$

However, $1-R_0$ must be positive for $b_2>0$ to hold true, which implies that $R_0<1$. Since $R_0<1$, the disease-free equilibrium of model (1) is locally asymptotically stable in Ω. □

3.6. Globally Stability of Disease Free-Equilibrium

Theorem 4. *If $R_0<1$, then the disease free-equilibrium point of system (1) is globally asymptotically stable in Ω.*

Proof. Take the Lyapunov function, as described by:

$$L=\frac{\delta}{(\delta+\sigma+\mu+\tau_1)(\theta+\sigma+\mu)}E+\frac{1}{(\theta+\sigma+\mu)}I, \quad (27)$$

where the DFE point (E_0) is in the open neighborhood defined by Ω. For equations $E(t)$ and $I(t)$, the Lyapunov function L is continuously differentiable, and $L>0$ for all $(E,I)\in\Omega$ as well as $L=0$ at DFE.

$$\begin{aligned} \frac{dL}{dt} &= \frac{\delta}{(\delta+\sigma+\mu+\tau_1)(\theta+\sigma+\mu)}\frac{dE}{dt}+\frac{1}{(\theta+\sigma+\mu)}\frac{dI}{dt}\\ &= \frac{\delta}{(\delta+\sigma+\mu+\tau_1)(\theta+\sigma+\mu)}\left[\beta SI-(\delta+\sigma+\mu+\tau_1)E\right]+\frac{1}{(\theta+\sigma+\mu)}\left[\delta E-(\theta+\sigma+\mu)I\right],\\ &\quad+\left[-\frac{\delta}{(\delta+\sigma+\mu+\tau_1)(\theta+\sigma+\mu)}(\delta+\sigma+\mu+\tau_1)+\frac{1}{(\theta+\sigma+\mu)}\delta\right]E,\\ &= \left[\frac{\delta\beta\pi}{(\delta+\sigma+\mu+\tau_1)(\theta+\sigma+\mu)\mu}-1\right]I+\left[-\frac{\delta}{(\theta+\sigma+\mu)}+\frac{\delta}{(\theta+\sigma+\mu)}\right]E,\\ &= \left[\frac{\delta\beta\pi}{(\delta+\sigma+\mu+\tau_1)(\theta+\sigma+\mu)\mu}-1\right]I. \end{aligned} \quad (28)$$

This implies that

$$\frac{dL}{dt}=[R_0-1]I. \quad (29)$$

Hence, $dL/dt\le 0$, we must have $R_0-1\le 0$. Thus, $dL/dt<0$ if $R_0<1$ and $dL/dt=0$ if and only if $I=0$. Therefore, the singleton set $E_0=(\pi/\mu,0,0,0,0)$ is the largest compact invariant set in $(E,I)\in\Omega$. As a result, every solution equations of model (1) with initial conditions in the Ω range approaches the disease-free equilibrium point as time (t) tends to infinity whenever $R_0<1$, according to Lasalle's invariant principle [29]. As a result, if $R_0<1$, the DFE pont is globally asymptotically stable in Ω. □

3.7. Endemic Equilibrium Point. The steady state solution where the disease continues to affect the population is the endemic equilibrium point, denoted by the symbol $E_1=(S^*,E^*,I^*,H^*,R^*)$. If we assume that the model's equilibrium point is typically (S^*,E^*,I^*,H^*,R^*), then model (1) gives;

$$
\begin{aligned}
S^* &= \frac{\pi + \omega R}{(R_0 - 1) + \mu},\\
E^* &= \frac{\pi(R_0 - 1)}{((R_0 - 1) + \mu)(\tau_1 + \delta + \sigma + \mu)},\\
I^* &= \frac{R_0 - 1}{\beta},\\
H^* &= \frac{\theta(R_0 - 1)}{(\tau_2 + \sigma + \mu)},\\
R^* &= \frac{(\tau_1\beta\pi I(\tau_2 + \sigma + \mu)) + \tau_2\theta I\mu(\tau_1 + \delta + \sigma + \mu)}{\mu(\tau_2 + \sigma + \mu)(\tau_1 + \delta + \sigma + \mu)}R_0.
\end{aligned}
\tag{30}
$$

It follows logically from the the above that whenever $R_0 > 1$, a unique positive endemic equilibrium point exists.

3.8. Globally Stability of Endemic Equilibrium

Theorem 5. *If $R_0 > 1$, then the endemic equilibrium point of the model equation (blue 1) is globally asymptotically stable.*

Proof. Consider the lyapunov function L defined by:

$$
L = \frac{1}{2}[(S - S^*) + (E - E^*) + (I - I^*) + (H - H^*) + (R - R^*)]^2. \tag{31}
$$

The partial derivative of (blue 24) with respect to time (t) corresponding to system (1) is obtain as,

$$
\begin{aligned}
\frac{\mathrm{d}L}{\mathrm{d}t} &= [(S - S^*) + (E - E^*) + (I - I^*) + (H - H^*) + (R - R^*)]\frac{\mathrm{d}}{\mathrm{d}t}[S + E + I + H + R]\\
&= [(S - S^*) + (E - E^*) + (I - I^*) + (H - H^*) + (R - R^*)]\frac{\mathrm{d}N}{\mathrm{d}t}.
\end{aligned}
\tag{32}
$$

Then, from the equations (5) we have,

$$
\frac{\mathrm{d}N}{\mathrm{d}t} = \frac{\mathrm{d}}{\mathrm{d}t}[S + E + I + H + R] \le \pi - \mu N. \tag{33}
$$

By substituting equations of model (33) into the equation (32), and the result is

$$
\begin{aligned}
\frac{\mathrm{d}L}{\mathrm{d}t} &= (S - S^*) + (E - E^*) + (I - I^*) + (H - H^*) + (R - R^*)\frac{\mathrm{d}}{\mathrm{d}t}[S + E + I + H + R],\\
&\le [(S - S^*) + (E - E^*) + (I - I^*) + (H - H^*) + (R - R^*)][\pi - \mu N],\\
&\le \left[N - \frac{\pi}{\mu}\right][\pi - \mu N].
\end{aligned}
\tag{34}
$$

We get the following result by rearranging and simplifying the equation (34).

$$
\frac{\mathrm{d}L}{\mathrm{d}t} \le -\frac{1}{\mu}[\pi - \mu N]^2. \tag{35}
$$

Hence, $(\mathrm{d}L/\mathrm{d}t)(S, E, I, H, R) \le 0$ and $\mathrm{d}L/\mathrm{d}t = 0$, if and only if $S^* = S$, $E^* = E$, $I^* = I$, $H^* = H$, and $R^* = R$. Therefore, the largest positive invariant set in $\{(S^*, E^*, I^*, H^*, R^*) \in \Omega: \mathrm{d}L/\mathrm{d}t = 0\}$ is a singleton E_1. Thus, E_1 is globally asymptotically stable in the set Ω in accordance to Lasalle's invariant principle [29]. □

4. Sensitivity Analysis

In this section, we have calculated the sensitivity analysis of parameters in the model (1), which affected the basic reproduction number in relation to parameter values in the Covid-19 model. Sensitivity analysis, as described in [30], for the basic reproductive number mainly helps to discover parameters that have a high impact on the values of R_0 and hence should be targeted for designing intervention strategy. These parameters can increase or decrease the basic reproduction number if their value increase or decrease and vice versa. Determine the normalized forward sensitivity index of the reproduction number regarding various model parameters in order to find the parameters that have a significant impact on the basic reproduction numbers R_0.

Definition 1. The normalized forward sensitivity index of R_0 that can be differentiable with respect to a particular parameter M is defined as [31, 32]

$$
k_M^{R_0} = \frac{\partial R_0}{\partial M} \times \frac{M}{R_0}. \tag{36}
$$

The sensitivity index of R_0 with respect to parameter β, for instance, is defined as follows:

$$k_{\beta}^{R_0} = \frac{\partial R_0}{\partial \beta} \times \frac{\beta}{R_0} = 0.5 > 0. \tag{37}$$

Using the same technique with respect to the parameters, $k_{\pi}^{R_0}$, $k_{\delta}^{R_0}$, $k_{\tau_1}^{R_0}$, $k_{\sigma}^{R_0}$, $k_{\mu}^{R_0}$, $k_{\theta}^{R_0}$ are computed and the sensitivity index are given in Table 2.

4.1. Interpretation of the Sensitivity Indices. The sensitivity indices of R_0 with respect to basic parameters are described in Table 2. This finding demonstrates how the parameters π,δ, and β have positive sensitivity indices that increase the value of R_0 as their values increase while the other parameters remain constant. And given that the μ,σ,τ_1 and θ parameters all have negative indices, increasing their values while holding the other parameters constant will decrease the value of R_0.

4.2. Parameter Estimations. In this section, we apply the suggested model to the total confirmed COVID-19 infection cases in Ethiopia and estimate the unknown model parameters using monthly cumulative data. Table 3 shows monthly data of all COVID-19 infection cases in Ethiopia from October 1, 2022, to October 30, 2022, taken from WHO situation reports (WHO, 2022).

We formulate system (1) in the following method to solve the dynamic parameter estimation problem:

$$\begin{aligned} z^{'} &= f(t, z, \theta), \\ z(t_0) &= z_0, \end{aligned} \tag{38}$$

where θ is the vector of unknown parameters and z is the vector of dependent variables. The sum of squares error (SSE) used to measure the error is represented by

$$\mathrm{SSE}(\theta) = \operatorname{argmin} \sum_{i=1} \left\| z_i(t) - \overline{z}_i(t) \right\|^2, \tag{39}$$

where n is the number of real data points that are available and $\|.\|$ represents the Euclidean norm in the variable R^n. The expression $z_i(t)$ is the corresponding model solution at time t_i, and the $\overline{z}_i(t)$ represents the actual total confirmed cases of COVID-19. During least-squares fitting, we seek a value for the model parameter θ such that the squared sum of errors is at its lowest. This value is $\overline{\theta}$. Given that the dependence of a solution $z(t, \theta)$ on the parameter θ is through a highly nonlinear system of differential equations, it is clear that this problem is a non-linearleast-squares problem.

As shown in Figure 2, the model parameters of system (1) are estimated using least-square fitting methods, which results in a better fit for the model solution to the real data. The corresponding parameter values are shown in Table 4.

As shown in Figure 2, the model solution fits the real data better when the model parameters of the model system (1) are estimated using least-square fitting methods. The corresponding parameter values are shown in the color blue table Table 4 below. The model's basic reproduction number estimate is given by the expression $R_0 = 2.64196 > 1$. The prevalence of COVID-19 will cause an epidemic because $R_0 > 1$.

5. Optimal Control Model

In this section, optimal control is a powerful mathematical tool that can be used to make decisions involving complex biological situations or reduce the number of exposed and infected people in the populations [34]. We extended a model (1) by incorporating three control measures to reduce COVID-19 transmissions. Thus, the following optimal control variables are provided: the control variable $u_1(t)$ represents the personal protection through the use of surgical face masks, social distance, isolation, and awareness of disease transmission whereas the control variable $u_2(t)$, represents the vaccination. Treatment for infected people is represented by the control variable $u_3(t)$. After incorporating the controls into the model (1), the optimal control model is formulated as follows:

$$\begin{cases} \dfrac{dS}{dt} = \pi - (1 - u_1)\beta IS - (u_2 + \mu)S + \omega R, \\ \dfrac{dE}{dt} = (1 - u_1)\beta IS - (\tau_1 + \delta + \sigma + \mu)E, \\ \dfrac{dI}{dt} = \delta E - (\theta + \sigma + \mu + u_3)I, \\ \dfrac{dH}{dt} = (\theta + u_3)I - (\tau_2 + \sigma + \mu)H, \\ \dfrac{dR}{dt} = \tau_1 E + \tau_2 H - (\mu + \omega)R. \end{cases} \tag{40}$$

In this optimal control problem, our main objective is to reduce the overall numbers of humans who have been exposed to and infected with COVID-19 in the population, while also reducing the overall cost of controlling the disease dynamics. The minimization problem's cost functional is what we refer to as:

$$J(u_1, u_2, u_3) = \min_{\substack{\Delta \\ u_1, u_2, u_3}} \int_0^{t_f} \mathrm{d}t, \left(A_1 E + A_2 I + \frac{1}{2}\left(B_1 u_1^2 + B_2 u_2^2 + B_3 u_3^2 \right) \right), \tag{41}$$

Table 2: Sensitivity indices of parameters.

Parameters symbol	Sensitivity index
π	0.5
δ	0.5
β	0.5
σ	−0.152158
μ	−0.152158
τ_1	−0.0315
θ	−0.4092

Table 3: Monthly e cases of COVID-19 in Ethiopia from October 1, 2022 to October 30, 2022.

No	Month	COVID-19 confirmed cases
1	1 October	493,587
2	2 October	493,588
3	3 October	493,616
4	4 October	493,627
5	5 October	493,640
6	6 October	493,654
7	7 October	493,671
8	8 October	493,682
9	9 October	493,684
10	10 October	493,698
11	11 October	493,708
12	12 October	493,723
13	13 October	493,738
14	14 October	493,767
15	10 October	493,781
16	16 October	493,783
17	17 October	493,783
18	18 October	493,803
19	19 October	493,818
20	20 October	493,837
21	21 October	493,837
22	22 October	493,864
23	23 October	493,875
24	24 October	493,885
25	25 October	493,894
26	26 October	493,905
27	27 October	493,912
28	28 October	493,937
29	29 October	493,939
30	30 October	493,940

Subject to the terms of the model system (40). The relative weight constant B_i measures the relative cost interventions associated with the control u_i for $i = 1,2,3$ and balances the units of integrand to reduce the dominance of any term in the integral. The expression $1/2B_iu_i^2$ stands for the cost function that corresponds to the controls $u_i(t)$, which is quadratic in accordance with the literature [27, 35, 36]. The positive constants A_1 and A_2 measure the relative importance of reducing the associated classes on the spread of the disease. To find the best possible control,

$$J(u_1^*, u_2^*, u_3^*) = \min\{J(u_1, u_2, u_3), u_1, u_2, u_3 \in \Omega\}, \quad (42)$$

where Ω the set of admissible control function as

$$\Omega = \left\{(u_1(.)u_2(.)u_3(.)); 0 \le u_1(t), u_2(t), u_3(t) \le 1 \forall t \in [0, t_f]\right\}, \quad (43)$$

is the control set subject to the model (40). All of the controls in this situation are bounded and measurable.

5.1. Existence of Optmal Control Problem. In this section, we establish the existence of an optimal control triples that optimize the objective functional specified in (41). As a consequence, we get the result below.

Theorem 6. *Given a cost functional $Ju_1,u_2,u_3)$ subject to control induced state system (40), then there exist an optimal control triples $u^* = (u_1^*,u_2^*,u_3^*)$ and the corresponding to the*

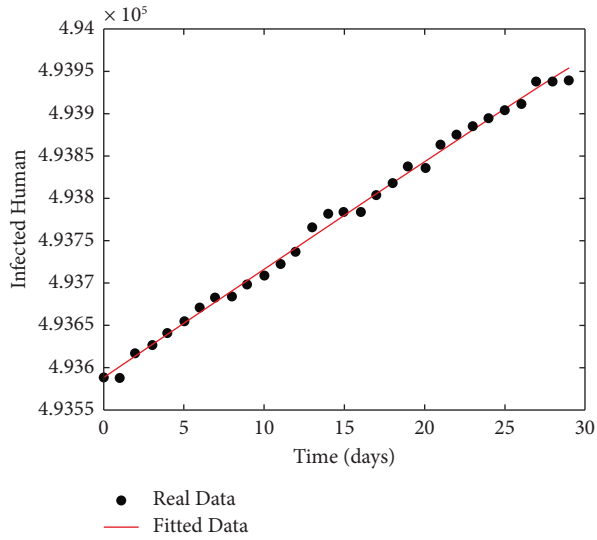

Figure 2: SEIHR model fit with real data on the number of COVID-19 cases in Ethiopia.

Table 4: Parameters from literature value and estimated values used for model (1).

Parameters	Estimated value	Reference
μ	0.0000301	Estimated
π	4995	Estimated
δ	0.000011618	[16]
σ	0.0218	Estimated
ω	1.2981	Estimated
β	0.38974	Estimated
τ_1	0.03232	Assumed
τ_2	0.6450	Estimated
θ	0.06813/day	[33]

optimal solution (S^*,E^*,I^*,H^*,R^*) *that minimize* $J(u)$ *over* Ω *such that*

$$J(u_1^*, u_2^*, u_3^*) = \min\{J(u_1, u_2, u_3): u_1, u_2, u_3 \in \Omega\}. \tag{44}$$

Proof. In order to show the existence of optimal controls triples, we must confirm the five terms listed below based on the result in [37].

(i) The set of controls and related state variables is non-empty.

(ii) The closed and convex measurable control set.

(iii) A linearized function in the state and control variables, depending on time and state variables, bounded the right side of the state system.

(iv) The cost functional integrand, $g(x,u)$, is convex on Ω.

(v) There exist constants $b_1, b_2 > 0$ and $b_3 > 1$ such that the integrand of the objective functional satisfies $g(x,u) \geq b_1(|u_1|^2, |u_2|^2, |u_3|^2)^{b_3/2} - b_2$.

(a) Take note that we have demonstrated the boundedness of the Covid-19 model (1). It follows that for all valid control functions in Ω, the state system solutions are continuous and bounded. Additionally, the Lipschitz condition is satisfied with regard to state variables by the right-hand side functions of the model equation (40). As a result, the system's (40) solutions are cited in [38]. As a result, the set Ω is not empty.

(b) Given that the control set $\Omega = [0,1]^3$, then Ω is closed by definition. Moreover, for any two points $y, z \in \Omega$ such that $y = (y_1, y_2, y_3)$ and $z = (z_1, z_2, z_3)$. By the definition of a convex set [39], for any $\lambda \in [0,1]$, it follows that $\lambda y_i + (1-\lambda)z_i \in \Omega_i, i = 1,2,3$. Hence, $\lambda y_i + (1-\lambda)z_i \in \Omega_i$ implies that Ω is convex set.

(c) The state system (41) is clearly linear in control variables u_1, u_2 and u_3 with coefficients depending on state variables. With this condition (iii) is satisfied.

(d) The integrand $g(t,x,u)$ of the cost functional is given by

$$g(t,x,u) = \underbrace{A_1E + A_2I}_{f(t,x)} + \underbrace{\frac{1}{2}\left(B_1u_1^2 + B_2u_2^2 + B_3u_3^2\right)}_{h(t,u)}. \tag{45}$$

Let $y=(y_1,y_2,y_3)$ and $z=(z_1,z_2,z_3)\in\omega$ and $\varpi\in[0,1]$. Then we have

$$\begin{aligned}h[t,\ (1-\varpi)y+\varpi z-((1-\varpi))h(t,\ y)+\varpi h(t,\ z)] &= \frac{B_1}{2}\left[(1-\varpi)^2y_1^2+2\varpi(1-\varpi)y_1z_1+\varpi^2z_1^2\right]\\ &+\frac{B_2}{2}\left[(1-\varpi)^2y_2^2+2\varpi(1-\varpi)y_2z_2+\varpi^2z_2^2\right]\\ &+\frac{B_3}{2}\left[(1-\varpi)^2y_3^2+2\varpi(1-\varpi)y_3z_3+\varpi^2z_3^2\right]\\ &=\left(\varpi^2-\varpi\right)\left(\frac{B_1}{2}(y_1-z_1)^2+\frac{B_2}{2}(y_2-z_2)^2+\frac{B_3}{2}(y_3-z_3)^2\right)\le 0.\end{aligned} \tag{46}$$

Hence,

$$h(t,\ (1-\varpi)y+\varpi z)\le(1-\varpi)h(t,y)+\varpi h_1(t,\ z), \tag{47}$$

which proves that $h(t,u)$ is a convex function [40]. Since the sum of two convex functions is convex, so that $g(t,x,u)$ is convex function.

(e) Lastly, we have

$$\begin{aligned}g(x,\ u) &= A_1E+A_2I+\frac{1}{2}\left(B_1u_1^2+B_2u_2^2+B_3u_3^2\right),\\ &\ge\frac{1}{2}\left(B_1u_1^2+B_2u_2^2+B_3u_3^2\right),\\ &\ge\frac{1}{2}\left(B_1u_1^2+B_2u_2^2+B_3u_3^2\right)^{b_3/2}-b_2,\end{aligned} \tag{48}$$

where $b_1=(1/2)\{\min B_1,B_2,B_3\}$, $b_2>0$ and $b_3=2$.

Hence, there exists an optimal control that minimizes the objective function. This completes the proof. □

5.2. Hamiltonian System. The Hamiltonian (H), which is made up of the state (40) and integrand of the objective functional (41), is required to drive the necessary condition. Pontryagin's minimum principle for the ideal control pair $(u_1^*,\ u_2^*,\ u_2^*)$ is given as follows.

$$H=\left[A_1E+A_2I+\frac{1}{2}\sum_{i=1}^{3}B_iu_i^2\right]+\lambda_i\left[\frac{\mathrm{d}S}{\mathrm{d}t}+\frac{\mathrm{d}E}{\mathrm{d}t}+\frac{\mathrm{d}I}{\mathrm{d}t}+\frac{\mathrm{d}H}{\mathrm{d}t}+\frac{\mathrm{d}R}{\mathrm{d}t}\right]. \tag{49}$$

Substituting (40) and (41) into (49) with respect to controls u_1, u_2, u_3 is given by

$$\begin{aligned}H&=\left[A_1E+A_2I+\frac{1}{2}\sum_{i=1}^{3}B_iu_i^2\right]\\ &+\lambda_1\left[\Lambda-(1-u_1)\beta IS-(u_2+\mu)S+\omega R\right],\\ &+\lambda_2\left[(1-u_1)\beta IS-(\tau_1+\delta+\sigma+\mu)E\right],\\ &+\lambda_3\left[\delta E-(\theta+\sigma+\mu+u_3)I\right],\\ &+\lambda_4\left[(\theta+u_3)I-(\tau_2+\sigma+\mu)H\right],\\ &+\lambda_5\left[\tau_1E+\tau_2H-(\mu+\omega)R\right],\end{aligned} \tag{50}$$

where λ_1, λ_2, λ_3, λ_4, and λ_5 are adjoint variables.

Theorem 7. *Let $u=(u_1,u_2,u_3)$ is optimal control with a unique optimal solution $(\widehat{S},\widehat{E},\widehat{I},\widehat{H},\widehat{R})$ of the optimal control problem (41) with a fixed time t_{tf} for all $t\in[0,\ t_{tf}]$. Moreover, there exist adjoint function λ_i for $i=1,2,3,4,5$ such that*

$$\begin{cases}\dfrac{\mathrm{d}\lambda_1}{\mathrm{d}t}=\beta I(1-u_1)(\lambda_1-\lambda_2)+\lambda_1(u_2+\mu),\\ \dfrac{\mathrm{d}\lambda_2}{\mathrm{d}t}=\lambda_2[\tau_1+\delta+\sigma+\mu]-\lambda_3\delta-\lambda_5\tau_1-A_1,\\ \dfrac{\mathrm{d}\lambda_3}{\mathrm{d}t}=(1-u_1)\beta S(\lambda_1-\lambda_2)+\lambda_3(\theta+\sigma+\mu+u_3)-\lambda_4(\theta+u_3)-A_2,\\ \dfrac{\mathrm{d}\lambda_4}{\mathrm{d}t}=\lambda_4(\tau_2+\sigma+\mu)-\lambda_5\tau_2,\\ \dfrac{\mathrm{d}\lambda_5}{\mathrm{d}t}=-\lambda_1\omega+\lambda_5(\omega+\mu).\end{cases} \tag{51}$$

With transiversality conditions $\lambda_i(t_f) = 0$ for $i = 1, 2, 3, 4, 5$. Furthermore, the optimal controls (u_1^*, u_2^*, u_3^*) are given by

$$u_1^* = \max\left\{0, \min\left\{1, \frac{\beta SI(\lambda_2 - \lambda_1)}{B_1}\right\}\right\}$$

$$u_2^* = \max\left\{0, \min\left\{1, \frac{\lambda_1 S}{B_2}\right\}\right\}, \tag{52}$$

$$u_3^* = \max\left\{0, \min\left\{1, \frac{-I(\lambda_4 - \lambda_3)}{B_3}\right\}\right\}.$$

Proof. The Hamiltonian function's derivative with respect to $S(t), E(t), I(t), H(t)$, and $R(t)$, respectively, is used to provide the form of the adjoint equation, which is then used to demonstrate the theorem. The adjoint equation is then provided by

$$\begin{cases} \frac{d\lambda_1}{dt} = \frac{-\partial H}{\partial S} = \beta I(1-u_1)(\lambda_1 - \lambda_2) + \lambda_1(u_2 + \mu), \\ \frac{d\lambda_2}{dt} = \frac{-\partial H}{\partial E} = \lambda_2[\tau_1 + \delta + \sigma + \mu] - \lambda_3\delta - \lambda_5\tau_1 - A_1, \\ \frac{d\lambda_3}{dt} = \frac{-\partial H}{\partial I} = (1-u_1)\beta S(\lambda_1 - \lambda_2) + \lambda_3(\theta + \sigma + \mu + u_3) - \lambda_4(\theta + u_3) - A_2, \\ \frac{d\lambda_4}{dt} = \frac{-\partial H}{\partial H} = \lambda_4(\tau_2 + \sigma + \mu) - \lambda_5\tau_2, \\ \frac{d\lambda_5}{dt} = \frac{-\partial H}{\partial R} = -\lambda_1\omega + \lambda_5(\omega + \mu), \end{cases} \tag{53}$$

with transiversality conditions $\lambda_i(t_f) = 0$ for $i = 1, 2, 3, 4, 5$.

The optimal control u_i^* is obtained by the optimality condition given by $\partial H/u_i = 0, i = 1,2,3,4,5$. Which implies that

$$\frac{\partial H}{\partial u_1} = \beta SI(\lambda_1 - \lambda_2) + B_1 u_1 = 0,$$

$$\frac{\partial H}{\partial u_2} = B_2 u_2 - \lambda_1 S = 0, \tag{54}$$

$$\frac{\partial H}{\partial u_3} = (\lambda_4 - \lambda_3)I + B_3 u_3 = 0.$$

The compact form of optimal controls $u = (u_1^*, u_2^*, u_3^*)$ can be written as

$$u_1^* = \max\left\{0, \min\left\{1, \frac{\beta SI(\lambda_2 - \lambda_1)}{B_1}\right\}\right\},$$

$$u_2^* = \max\left\{0, \min\left\{1, \frac{\lambda_1 S}{B_2}\right\}\right\}, \tag{55}$$

$$u_3^* = \max\left\{0, \min\left\{1, \frac{-I(\lambda_4 - \lambda_3)}{B_3}\right\}\right\}.$$

In the next part, we will see the numerical simulation of optimality system to identify an optimum and least cost strategy for controlling the dynamics of COVID-19. □

6. Numerical Simulation

In this section, we will see the numerical simulation to show the model's dynamical characteristics, the stability of the equilibrium points, and a sensitivity analysis. We perform numerical simulation on the model (1) using MATLAB software, estimating the values of the model's basic parameters. Next, we graphically display the simulation results. We demonstrate numerically how to solve the optimal control problem proposed in system (40) and explain how a control strategy affects the spread of corona virus diseases. We employ a Runge-Kutta fourth order and the forward-backward sweep technique described in Lenhart and Workman's book [34]. The cost coefficients for the control variables are predicted to be $B_1 = 60, B_2 = 100$, and $B_3 = 80$, while the relative importance of reducing the associated classes on the spread of the disease is predicted to be $A_1 = 80$ and $A_2 = 60$. We analyze and compare the numerical results of the impact of controls on the dissemination of COVID-19 in populations using all pertinent information from the aforementioned sources.

6.1. Strategy A: Combination of Protective (u_1) and Vaccination (u_2). The controls for personal protection u_1 and vaccination u_2 in this strategy in order to maximize the objective functional $J(u)$, with the value of the treatment of infected individuals (u_3) set to zero. The exposed and infected plots demonstrated the effectiveness of the strategy under consideration. The numerical results shown in Figure 3(a) below show that the number of COVID-19-infected populations is increasing quickly in the absence of control strategies, while it is decreasing and finally reaching a halt in the presence of u_1 and u_2 controls. We deduced from the second numerical result shown in Figure 3(b) below experimented that the number of COVID-19 exposed individuals is rapidly increasing in the absence of control strategies, while the number of exposed populations is decreasing at the end of the experiment in the presence of u_1 and u_2 controls. As a result, while this strategy is effective at reducing the number of exposed people, it is less effective at doing so. Figure 3(c) also shows the control profiles u_1 and u_2, which come to the conclusion that personal protective control u_1 controls maintain upper bound (100%) for 175 days while vaccination control u_2 controls reach maximum level (95%) in 150 days.

6.2. Strategy B: Combination of Protective (u_1) and Treatment (u_3). In this case, personal protection control (u_1) and infection treatment (u_3) have been used to reduce the objective functional $J(u)$, while the control vaccination (u_2) has been set to zero. According to the numerical results in Figure 4(a) blow, the overall number of COVID-19-infected humans is decreasing in the presence of control while rapidly increasing in the absence of control. According to the second numerical result in Figure 4(b), COVID-19 exposed rates are decreasing in the presence of controls while rising in the absence of controls. The control profiles u_1 and u_3 are plotted in Figure 4(c), and they indicate that controls on personal protective measures u_1 and the treatment of infected people u_3 should maintain an upper bound of 100% throughout the intervention period.

6.3. Strategy C: Combination of Vaccination (u_2) and Treatment of Infected (u_3). In order to reduce the objective functional $J(u)$, we simulated the model using control vaccination (u_2) and treatment of infected (u_3), with personal protection (u_1) set to zero. From the numerical results shown in Figure 5(a), we deduced that the number of COVID-19-infected populations is rapidly rising in the absence of control strategies, while it is falling in the presence of controls. From the second numerical result displayed in Figure 5(b), we deduced that the number of exposed populations of COVID-19 are increasing in the absence of controls, while decreasing in the presence of controls. The control profiles u_2 and u_3 are also shown in Figure 5(c). The control profiles u_2 and u_3 come to the conclusion that the vaccination control u_2 is at its maximum level (95%) in 150 days and the treatment of infected u_3 is maintained at its maximum level (100%) until the end of the implementation.

6.4. Strategy D: Applying All Control Strategies. To reduce the objective functional $J(u)$, we have used all three control interventions in this instance on each compartment. Figures 6(a) and 6(b) show that the total of infected and exposed population decreases in the presence of controls while increasing in the absence of controls. Additionally, the control profile shown in Figure 6(c) demonstrates that the control u_1 and u_3 are at their highest level (100%) in every days and the control u_2 is at maximum level (95%) in 150 days. In all of the above strategies, this control profile's u_1 and u_3 interpretation is the same.

7. Cost Effectiveness Analysis

In this section, in order to demonstrate the intervention that was used to minimize the spread of COVID-19, we must demonstrate the most efficient and less costly strategy with cost-effective analysis. The incremental cost effectiveness ratio (ICER) for two strategies, i and j, as calculated by [41–43] is used to investigate cost effectiveness analysis and givens as

$$\text{ICER} = \frac{\text{Change in total averted costs between two strategies i and j}}{\text{Change in total number of infections averted between two strategies i and j}}. \tag{56}$$

The total number of people averted is calculated by subtracting the total number of new cases with control from the total number of new cases without control using numerical simulation results from the COVID-19 model (40). Utilizing each strategy's specific cost functions $1/2B_1u_1^2$, $1/2B_2u_2^2$ and $1/2B_3u_3^2$ [23, 44], it is possible to determine the total cost of each strategy over the course of the intervention.

The estimated total number of people averted in increasing order and the total cost are listed in Table 5 based on simulations of the system (31) using the values of parameters in Table 4.

Applying ICER techniques, we used the value in Table 5 the number of people averted and total cost of each strategy as obtained to compare two intervention strategies. The

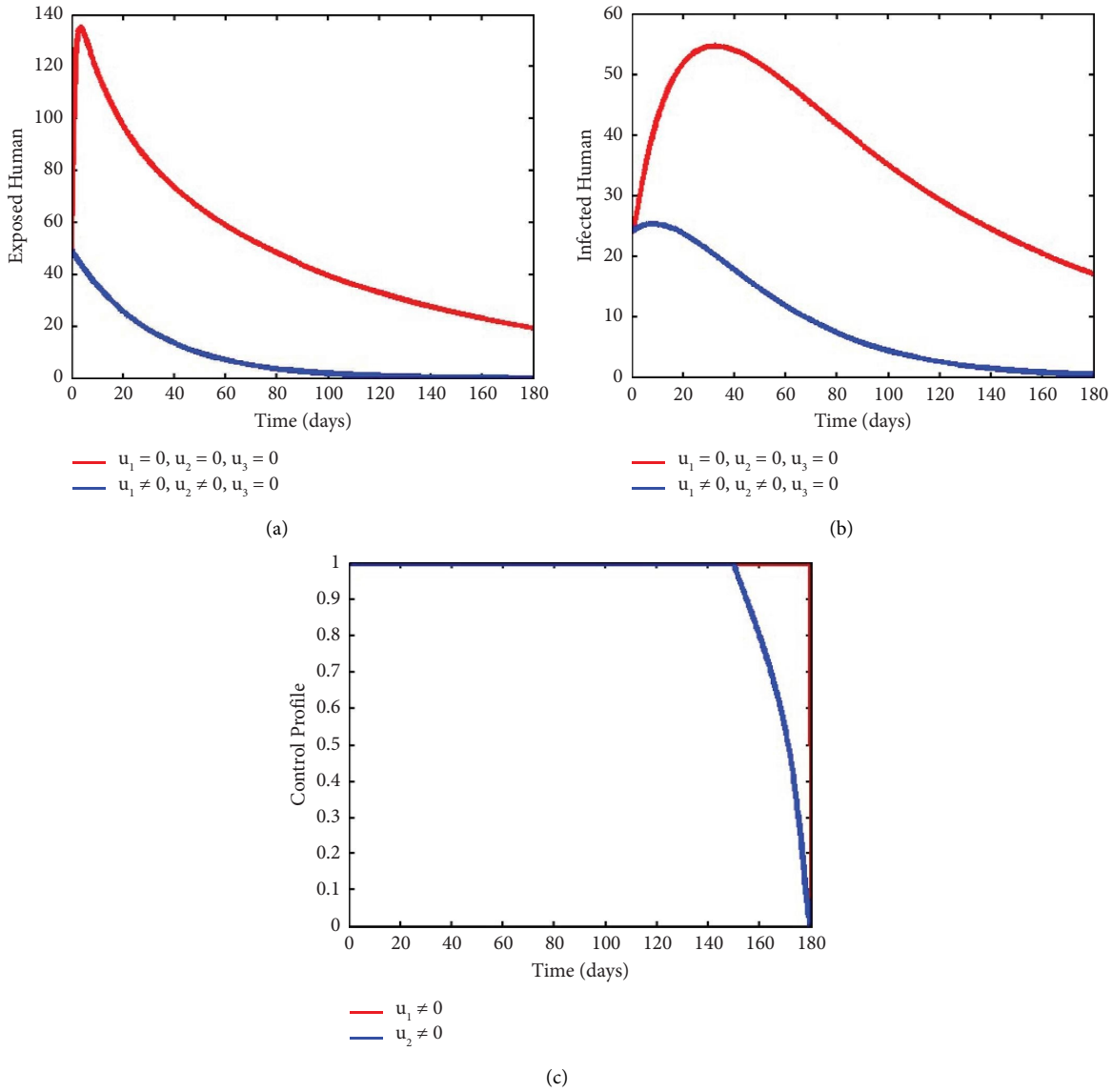

Figure 3: Simulation result with strategy of personal protection u_1 and vaccination u_2.

incremental cost effectiveness ratio (ICER) for the each competing strategies is estimated as obtained as

$$\begin{aligned}
\text{ICER}(A) &= \frac{50,797.317}{26,406.92} = 1.924,\\
\text{ICER}(C) &= \frac{62,900.205 - 50,797.317}{35,404.79 - 26,406.92} = 1.345,\\
\text{ICER}(D) &= \frac{66,683.279 - 62,900.205}{35,659.43 - 35,404.79} = 14.8566,\\
\text{ICER}(B) &= \frac{69,862.7575 - 66,683.279}{35,906.19 - 35,659.43} = 12.884.
\end{aligned} \tag{57}$$

The total number of individuals averted by Strategies A, C, D, and B in increasing order along with the total cost are shown in Table 6.

When A and C are compared in Table 6, ICER (C) is lower than ICER (A). This suggests that strategy A is expensive and less effective at saving people. As a result, strategy C dominates more than strategy A. As a result, we eliminated strategy A from the competing strategies. Then, as shown in Table 7, compute the ICER once more for the other strategies C, D, and B.

The comparison between the intervention strategies C and D shows that the ICERC is lower than the ICERD in Table 7. This demonstrates that strategy C saves more people than strategy D. As a result, we have omitted the strategy d from a group of competing strategies as well as the ICER as shown in Table 8.

The comparison of the two intervention strategies, C and B, in Table 8, demonstrates that ICER (C) is less than ICER (B). This suggests that strategy C more dominates than strategy B. So that the least expensive overall and most

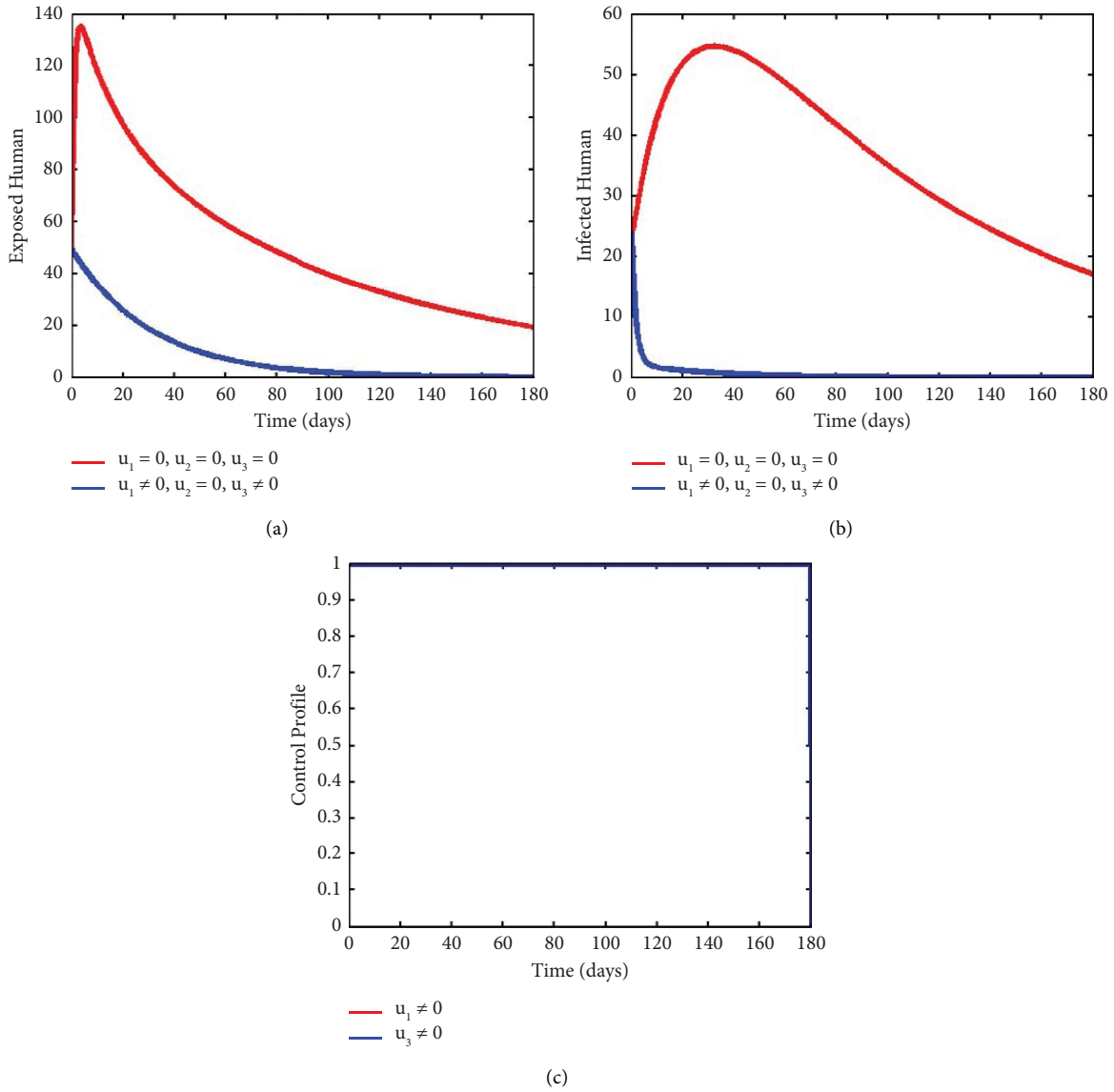

Figure 4: Simulation strategy of personal protection u_1 and treatment of infected u_3.

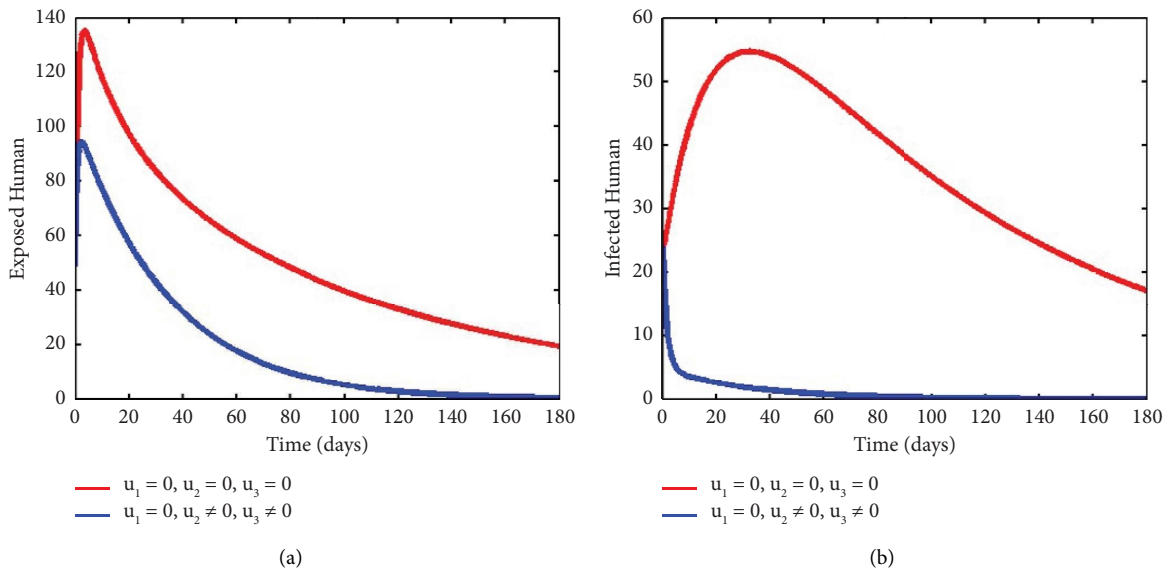

Figure 5: Continued.

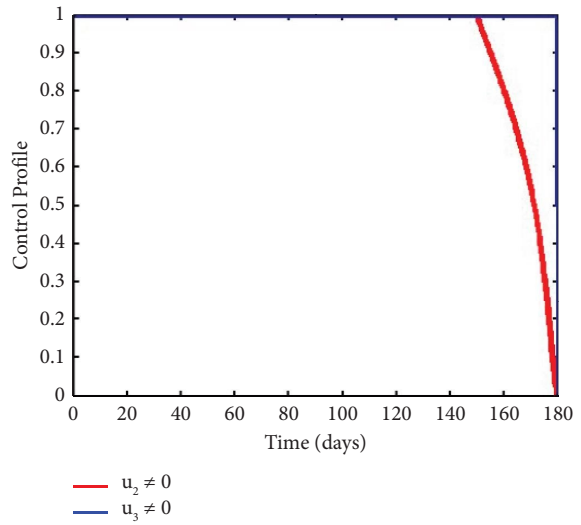

(c)

Figure 5: Simulation result with strategy of vaccination u_2 and treatment of infected u_3.

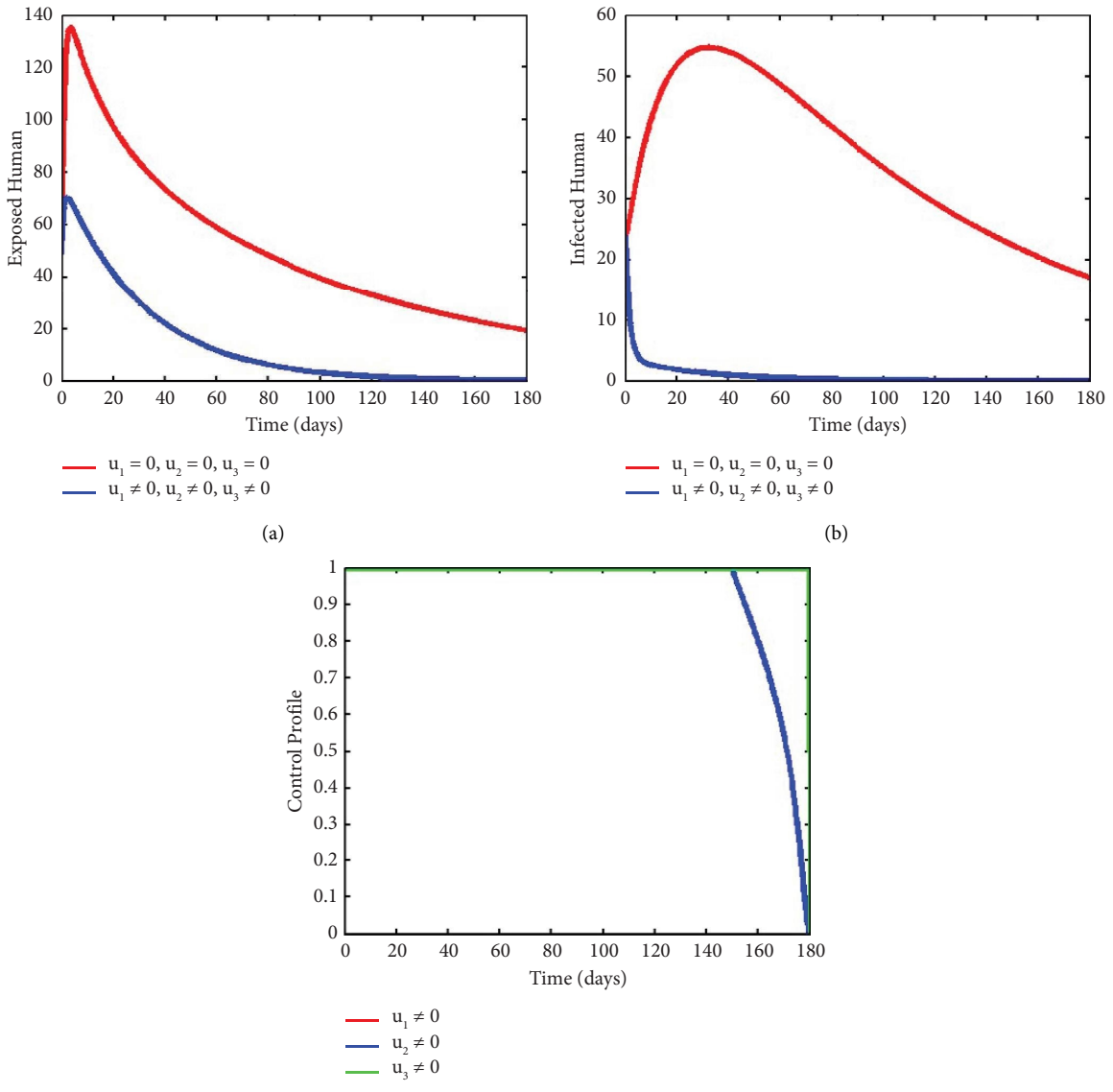

(a) (b)

(c)

Figure 6: Simulation result with all control strategies u_1,u_2 and u_3.

Table 5: Total amount of infection averted and total cost for all strategies.

Strategies	Total infections averted	Total cost ($)
Strategy A	26,406.92	50,797.317
Strategy C	35,404.79	62,900.205
Strategy D	35,659.43	66,683.279
Strategy B	35,906.19	69,862.7575

Table 6: Total amount of infection averted and total cost for all strategies.

Strategies	Total infections averted	Total cost ($)	ICER
Strategy A	26,406.92	50,797.317	1.924
Strategy C	35,404.79	62,900.205	1.345
Strategy D	35,659.43	66,683.279	14.8566
Strategy B	35,906.19	69,862.7575	12.884

Table 7: Amount of the total infection averted and total cost used with ICER.

Strategies	Amount of infections saved	Total cost ($)	ICER
C	35,404.79	62,900.205	1.345
D	35,659.43	66,683.279	14.8566
B	35,906.19	69,862.7575	12.884

Table 8: Amount of the total infection averted and total cost used with ICER.

Strategies	Amount of infections saved	Total cost ($)	ICER
C	35,404.79	62,900.205	1.345
B	35,906.19	69,862.7575	12.884

effective strategy was C. As a result of the analysis, we advise that the best and least expensive method for reducing the spread of COVID-19 is intervention C, which implies a combination of vaccination and treatment of infected individuals.

8. Conclusion

In this paper, we analyzed a deterministic mathematical model of the COVID-19 vaccine epidemic with optimal control model. We first obtained the feasible region where the model is epidemiologically and mathematically well-posed. Then the basic reproduction number with respect to the disease-free equilibrium point is computed using the next-generation matrix method. We then analyzed both local and global stability of the disease free equilibrium point based on basic reproduction number. Using the Jacobian matrix and the Lyapunov method, respectively, the disease-free equilibrium point is both locally and universally stable if the basic reproduction number is less than unity. The endemic equilibrium point exists when the basic reproduction number is greater than one. The model's sensitivity analysis has been investigated. In Parameter estimation, the model parameters are fitted using COVID-19 infected data reported from October 1, 2022 to October 30, 2022 in Ethiopia. The model was expanded to the problem of optimal control using three controls, namely personal protection, immunization, and treatment infection for reducing novel coronavirus diseases. Besides, with all combinations of the three controls, the optimal control model applies the Pontraygin's maximum principle and uses cost effectiveness analysis to determine the minimal cost using incremental cost effectiveness ratio (ICER). The outcome of the numerical simulation indicated that every control factor that was taken into account in the simulation helped to lower COVID-19 infections. The combination of vaccination and treatment for infected individuals is the best strategy, to effectively reduce the COVID-19 disease, according to the results of simulation with optimal control and cost effectiveness analysis.

Data Availability

The data used to support the findings of this study are available from the corresponding author upon request.

Conflicts of Interest

The authors declare that they have no reported conflicts of interest on the publication of this article.

References

[1] E. Dong, J. Ratcliff, T. D. Goyea et al., "The johns hopkins university center for systems science and engineering covid-19 dashboard: data collection process, challenges faced, and lessons learned," *The Lancet Infectious Diseases*, vol. 9, 2022.

[2] WHO, "Global situation," 2022, https://covid-19.who.int/.

[3] Covid1, "Nigeria centre for disease control," 2020, https://covid19.ncdc.gov.ng/faq/.

[4] A. S. Oke, O. I. Bada, G. Rasaq, and V. Adodo, "Mathematical analysis of the dynamics of COVID-19 in Africa under the influence of asymptomatic cases and re-infection," *Mathematical Methods in the Applied Sciences*, vol. 45, no. 1, pp. 137–149, 2022.

[5] B. Yang, Z. Yu, and Y. Cai, "The impact of vaccination on the spread of COVID-19: studying by a mathematical model," *Physica A: Statistical Mechanics and its Applications*, vol. 590, Article ID 126717, 2022.

[6] A. Abriham, D. Dejene, T. Abera, and A. Elias, "Mathematical mathematical modeling for COVID-19 transmission dynamics and the impact of prevention strategies: a case of ethiopiaodeling for COVID-19 transmission dynamics and the impact of prevention strategies: a case of Ethiopia," *International Journal of Mathematics and Soft Computing*, vol. 7, pp. 43–59, 2021.

[7] O. P. Noah and D. M. Kabir, "A mathematical model of COVID-19 infection transmission dynamics," *KASU Journal of Mathematical Science*, vol. 2, no. 2, pp. 57–73, 2021.

[8] I. Ahmed, G. U. Modu, A. Yusuf, P. Kumam, and I. Yusuf, "A mathematical model of Coronavirus Disease (COVID-19) containing asymptomatic and symptomatic classes," *Results in Physics*, vol. 21, Article ID 103776, 2021.

[9] M. H. DarAssi, M. A. Safi, M. A. Khan, A. Beigi, A. A. Aly, and M. Y. Alshahrani, "A mathematical model for SARS-CoV-2 in variable-order fractional derivative," *The European Physical Journal - Special Topics*, vol. 231, pp. 1905–1914, 2022.

[10] O. J. Peter, S. Qureshi, A. Yusuf, M. Al-Shomrani, and A. A. Idowu, "A new mathematical model of COVID-19 using real data from Pakistan," *Results in Physics*, vol. 24, Article ID 104098, 2021.

[11] R. W. Mbogo, J. W. W. Odhiambo, and J. W. Odhiambo, "COVID-19 outbreak, social distancing and mass testing in Kenya-insights from a mathematical model," *Afrika Matematika*, vol. 32, no. 5-6, pp. 757–772, 2021.

[12] S. Khajanchi, K. Sarkar, J. Mondal, K. S. Nisar, and S. F. Abdelwahab, "Mathematical modeling of the COVID-19 pandemic with intervention strategies," *Results in Physics*, vol. 25, Article ID 104285, 2021.

[13] N. K. Goswami and B. Shanmukha, "Dynamics of COVID-19 outbreak and optimal control strategies: a model-based analysis," *Advances in Systems Science and Applications*, vol. 21, no. 4, pp. 65–86, 2021.

[14] M. Nana-Kyere and E. O. Sacrifice, "Compartmental SEIRW COVID-19 optimal control model," *Communications in Mathematical Biology and Neuroscience*, vol. 2020, 2020.

[15] B. Seidu, "Optimal strategies for control of COVID-19: optimal strategies for control of COVID-19: a mathematical perspective mathematical perspective," *Scientifica*, vol. 2020, Article ID 4676274, 12 pages, 2020.

[16] A. I. Abioye, O. J. Peter, H. A. Ogunseye et al., "Mathematical model of COVID-19 in Nigeria with optimal control," *Results in Physics*, vol. 28, Article ID 104598, 2021.

[17] S. E. Moore and O. Eric, "Controlling the transmission dynamics of COVID-19," 2020, https://arxiv.org/abs/2004.00443.

[18] L. L. Obsu and S. F. Balcha, "Optimal control strategies for the transmission risk of COVID-19," *Journal of Biological Dynamics*, vol. 14, no. 1, pp. 590–607, 2020.

[19] J. K. K. Asamoah, E. Okyere, A. Abidemi et al., "Optimal control and comprehensive cost-effectiveness analysis for COVID-19," *Results in Physics*, vol. 33, Article ID 105177, 2022.

[20] R. Maryam, "Optimal control of a seir model with confinement of COVID'19," *The Journal OA*, vol. 11, no. 5, pp. 5447–5457, 2021.

[21] C. T. Deressa and G. F. T. Duressa, "Modeling and optimal control analysis of transmission dynamics of COVID-19: modeling and optimal control analysis of transmission dynamics of COVID-19: the case of Ethiopiahe case of Ethiopia," *Alexandria Engineering Journal*, vol. 60, no. 1, pp. 719–732, 2021.

[22] T. Li, Y. Guo, and Y. Guo, "Modeling and optimal control of mutated COVID-19 (Delta strain) with imperfect vaccination," *Chaos, Solitons and Fractals*, vol. 156, Article ID 111825, 2022.

[23] S. Olaniyi, O. S. Obabiyi, K. O. Okosun, A. T. Oladipo, and S. O. Adewale, "Mathematical modelling and optimal cost-effective control of COVID-19 transmission dynamics," *The European Physical Journal Plus*, vol. 135, no. 11, p. 938, 2020.

[24] C. S. Bornaa, B. Seidu, Y. I. Seini, B. Seidu, and Y. Ibrahim Seini, "Modeling the impact of early interventions on the transmission dynamics of coronavirus infection," *F1000Research*, vol. 10, p. 518, 2021.

[25] H. W. W. Hethcote, "The mathematics of infectious diseases," *SIAM Review*, vol. 42, no. 4, pp. 599–653, 2000.

[26] P. Van den Driessche and J. Watmough, "Reproduction numbers and sub-threshold endemic equilibria for compartmental models of disease transmission," *Mathematical Biosciences*, vol. 180, no. 1-2, pp. 29–48, 2002.

[27] T. D. Keno, L. B. Dano, and G. A. Ganati, "Optimal control and cost-effectiveness strategies of malaria transmission with impact of climate variability," *Journal of Mathematics*, vol. 33, 2022.

[28] L. B. Dano, K. P. Rao, T. D. Keno, and K. P. Rao, "Fractional order differential equations for chronic liver cirrhosis with frequent hospitalization," *BMC Research Notes*, vol. 15, no. 1, pp. 332–410, 2022.

[29] J. P. La Salle, "The stability of dynamical systems," *Society for Industrial and Applied Mathematics*, vol. 1, 1976.

[30] T. D. Keno, O. D. Makinde, and L. L. Obsu, "Optimal optimal control and cost effectiveness analysis of SIRS malaria disease model with temperature variability factorontrol and cost effectiveness analysis of SIRS malaria disease model with temperature variability factor," *Journal of Mathematical and Fundamental Sciences*, vol. 53, no. 1, pp. 134–163, 2021.

[31] L. B. Dano, K. P. Rao, T. D. Keno, K. P. Rao, and T. D. Keno, "Modeling the modeling the combined effect of hepatitis B infection and heavy alcohol consumption on the progression dynamics of liver cirrhosisombined effect of hepatitis B infection and heavy alcohol consumption on the progression dynamics of liver cirrhosis," *Journal of Mathematics*, vol. 2022, Article ID 6936396, 18 pages, 2022.

[32] T. D. Keno, O. D. Makinde, L. L. Obsu, and M. Daniel, "Impact of temperature variability on SIRS malaria disease model," *Journal of Biological Systems*, vol. 29, no. 3, pp. 773–798, 2021.

[33] M. A. Khan, A. Atangana, E. Alzahrani, A. Atangana, and E. Alzahrani, "The dynamics of COVID-19 with quarantined and isolation," *Advances in Difference Equations*, vol. 2020, no. 1, pp. 425–522, 2020.

[34] S. Lenhart and J. T. Workman, *Optimal Control Applied to Biological Models*, Chapman and Hall/CRC, New York, NY, USA, 2007.

[35] S. Ullah, M. A. Khan, and M. A. Khan, "Modeling the impact of non-pharmaceutical interventions on the dynamics of novel coronavirus with optimal control analysis with a case study," *Chaos, Solitons and Fractals*, vol. 139, Article ID 110075, 2020.

[36] Z. H. Shen, Y. M. Chu, M. A. Khan, S. Muhammad, O. A. Al-Hartomy, and M. Higazy, "Mathematical modeling and optimal control of the COVID-19 dynamics," *Results in Physics*, vol. 31, Article ID 105028, 2021.

[37] W. H. Fleming and R. Rishel, "Optimal deterministic and stochastic control," *Applications of Mathematics*, Springer, Berlin, Germany, 1975.

[38] D. L. Lukes, *Differential Equations, ser.*" *Mathematics in Science and Engineering*, Academic Press Inc.Harcourt Brace Jovanovich Publishers, London, UK, 1982.

[39] A. Beck, *Introduction to Nonlinear Optimization: Theory, Algorithms, and Applications with MATLAB*, Society for

Industrial and Applied Mathematics, Philadelphia, PA, USA, 2014.

[40] E. K. Chong and S. H. Zak, *An Introduction to Optimization*, John Wiley and Sons, Hoboken, NJ, USA, 2004.

[41] J. O. Akanni, F. O. Akinpelu, S. Olaniyi, A. T. Oladipo, and A. W. Ogunsola, "Modelling financial crime population dynamics: optimal control and cost-effectiveness analysis," *International Journal of Dynamics and Control*, vol. 8, no. 2, pp. 531–544, 2020.

[42] F. M. Legesse, K. P. Rao, and T. D. Keno, "Mathematical modeling of a bimodal pneumonia epidemic with non-breastfeeding class," *Applied Mathematics & Information Sciences An International Journal*, vol. 17, no. 1, pp. 95–107, 2023.

[43] T. D. Keno, O. D. Makinde, and L. L. Obsu, "Modelling and optimal control analysis of malaria epidemic in the presence of temperature variability," *Asian-Europian Journal of Mathematics*, vol. 15, no. 1, 2022.

[44] T. D. Keno, L. B. Dano, O. D. Makinde, and M. Daniel, "Modeling and modeling and optimal control analysis for malaria transmission with role of climate variabilityptimal control analysis for malaria transmission with role of climate variability," *Computational and Mathematical Methods*, vol. 2022, Article ID 9667396, 18 pages, 2022.